JOURNAL OF MATERIALS SCIENCE 28 (1993) 3754–3760

Influence of production conditions on the densification of zirconia powders obtained from acetates

M. DESCEMOND, C. BRODHAG, F. THEVENOT
Ecole Nationale Supérieure des Mines de Saint Etienne, 158 Cours Fauriel, 42023 Saint Etienne Cedex 2, France

B. DURAND, M. ROUBIN
Laboratoire de Chimie Minérale 3, URA CNRS no. 116, ISIDT, Université Claude Bernard Lyon I, 43 Boulevard du 11 November 1918, 69622 Villeurbanne Cedex, France

A. SAMDI
Faculté des Sciences Aïn Chok, BP 5366, Maarif, Casablanca, Morocco

Tetragonal yttrium-stabilized zirconia samples were obtained by pyrolysis of amorphous acetates containing both metals, at 950 °C in air. The dilatometric behaviour of samples indicates a dedensification when pyrolysis is carried out with a non-linear heating rate causing an absence of fine open porosity. A destabilization when cooling is observed for samples exhibiting a wide granulometry with agglomerate sizes reaching 100 μm. Even when neither one, nor the other phenomenon is noticed, an important aggregation state of the starting powders limits the densification and leads to poor sintered densities.

1. Introduction

According to former studies, finely grained pure zirconia may be prepared by pyrolysis of either crystallized [1] or amorphous [2] zirconium acetates, whereas yttrium-stabilized zirconia can be obtained only by pyrolysis of amorphous acetates containing both yttrium and zirconium [3], the pyrolysis of crystallized acetates leading to mixtures of zirconia and yttrium oxide [4]. This paper reports a study of the densification of yttrium-stabilized zirconia formed by pyrolysis of amorphous acetates, synthesized following the previously proposed procedure [3].

2. Preparation of zirconia powders

All samples were prepared from commercial zirconyl acetate solutions containing 300 $g l^{-1}$ ZrO_2 (Hoechst or Magnesium Elektron) to which the required amount of yttrium was added in the form of yttrium acetate dissolved in a 1/1 water–ethanoic acid solution, in order to obtain yttrium-stabilized zirconia with a ratio $Y_2O_3/(Y_2O_3 + ZrO_2) = 2.5$–3 or 3.5 mol %. The concentrated mixture was then diluted and neutralized to pH 7 with an ammonia solution. The amorphous acetate was finally obtained, with one exception, by evaporating solutions on a sand bath at 90 °C. According to the dilution and the neutralization procedure, three groups of samples may be distinguished (Fig. 1).

It was chosen to carry out pyrolysis at 950 °C because an EPR study of amorphous zirconium acetates showed that the paramagnetic signal induced by the presence of carbon residues in zirconia disappeared between 850 and 950 °C [2].

3. Powders characterization

3.1. Granulometric and morphological characterization

The size of agglomerates was determined with alcoholic suspensions using a laser granulometer. The cumulated frequency curves (Fig. 2) indicate that Samples 4, 5, 6 and 7, exhibiting median diameters of ~20 μm, are coarser grained powders than Samples 1, 2, 3, 8 and 9. Sample 8 is the finest powder.

The morphology of powders was also investigated by scanning electron microscopy, dry powders being deposited on a support without preliminary liquid dispersion. Samples 1, 2, 3 and 8 show a wide granulometry with a mean agglomerates size close to several tens of micrometres (Fig. 3a). Either very small particles (< 1 μm) or very large agglomerates (up to 100 μm) are observed particularly for Sample 8. These large agglomerates do not appear on the granulometric curves except for Sample 1. They are probably broken by the liquid dispersion. Samples 4, 5, 6, 7 and 9 present a narrow granulometry with a mean agglomerates size close to several tens of micrometres in accordance with granulometric analysis (Fig. 3b).

0022–2461

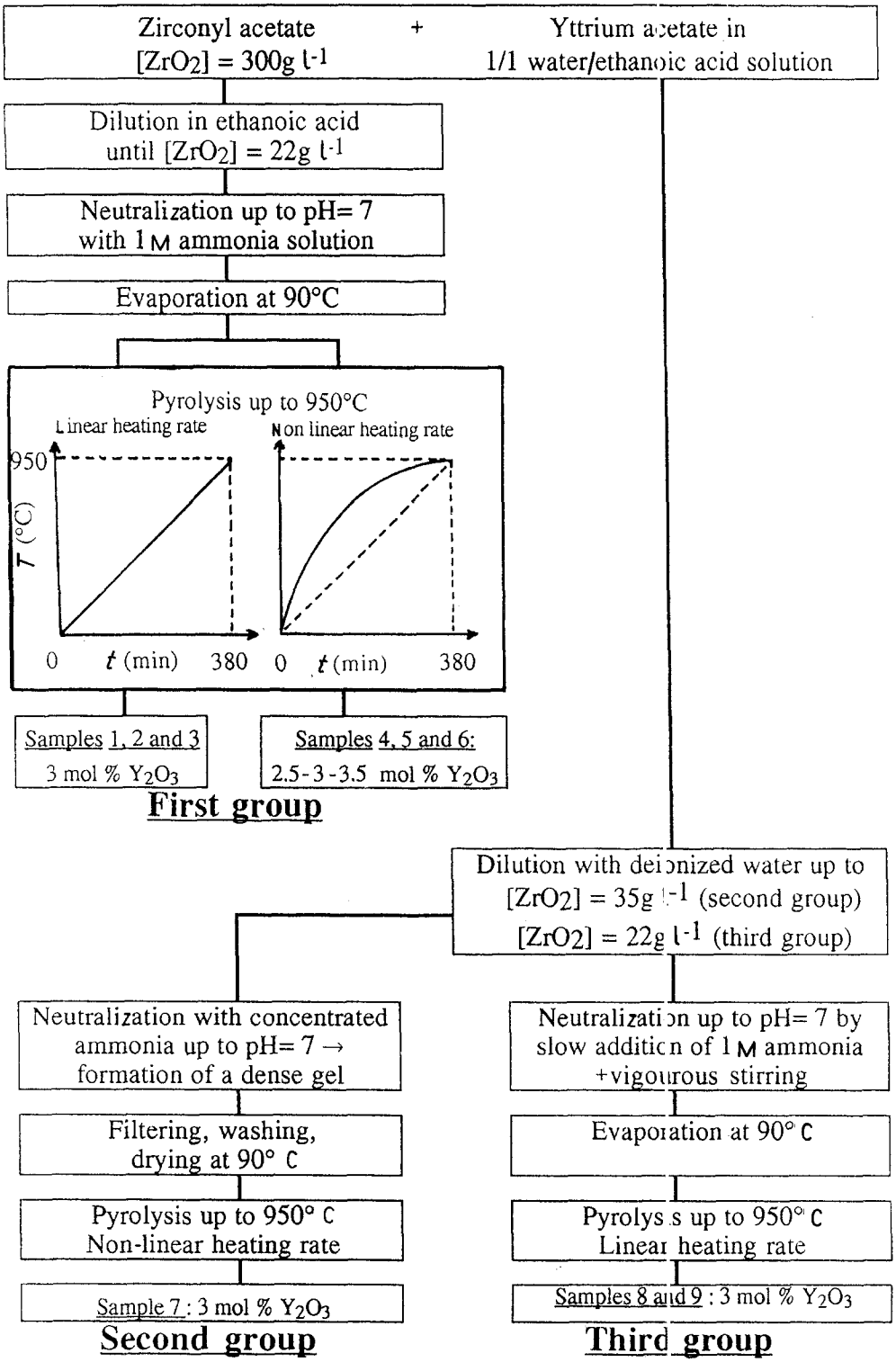

Figure 1 Zirconia sample preparation procedure. Samples 1, 2 and 3 differ in the starting acetate solution. Samples 8 and 9 were prepared by the same procedure at two different time periods.

3.2. Porosity measurements

The porosity of powders was measured on pellets, prepared by uniaxial pressing at 400 MPa, by mercury penetration up to a pressure of 200 MPa. Porous volumes were always in the vicinity of 120 $mm^3 g^{-1}$, but powders could be separated into two groups according to the pore-size distribution and the specific surface area.

The first group, Samples 1, 2 and 3, was characterized by specific surface areas close to 5 $m^2 g^{-1}$ and by bimodal size distributions (Table I, Fig. 4). The largest part of the porous volume was constituted by pores, the size of which is included in the range 0.02–2.50 μm with a maximum at 0.90 μm. The other part was made up of very narrow pores with sizes in the range 4.0–7.5 nm.

The second group, Samples 4, 5, 6 and 7, was characterized by lower specific surface areas, principally for Samples 4, 5 and 6, and regular size distribution (Table II, Fig. 4). The porous volume is constituted by larger pores, the size of which is in the range 0.2–7.5 μm with a maximum frequently ex-

TABLE I Porosity characterization of Samples 1, 2 and 3

Sample	Total porous volume ($mm^3\ g^{-1}$)	Specific surface area ($m^2\ g^{-1}$)	$d > 0.1\ \mu m$			$d < 0.1\ \mu m$	
			Porous volume ($mm^3\ g^{-1}$)	Pore size (μm)	Peak maximum (μm)	Porous volume ($mm^3\ g^{-1}$)	Pore size ($10^{-3}\ \mu m$)
1	115	4.2	106	0.02–2.50	0.7	9	4.00–7.50
2	127	4.6	120	0.02–2.50	0.6	7	4.00–6.00
3	123	6.8	108	0.02–2.00	0.9	14	4.00–9.00

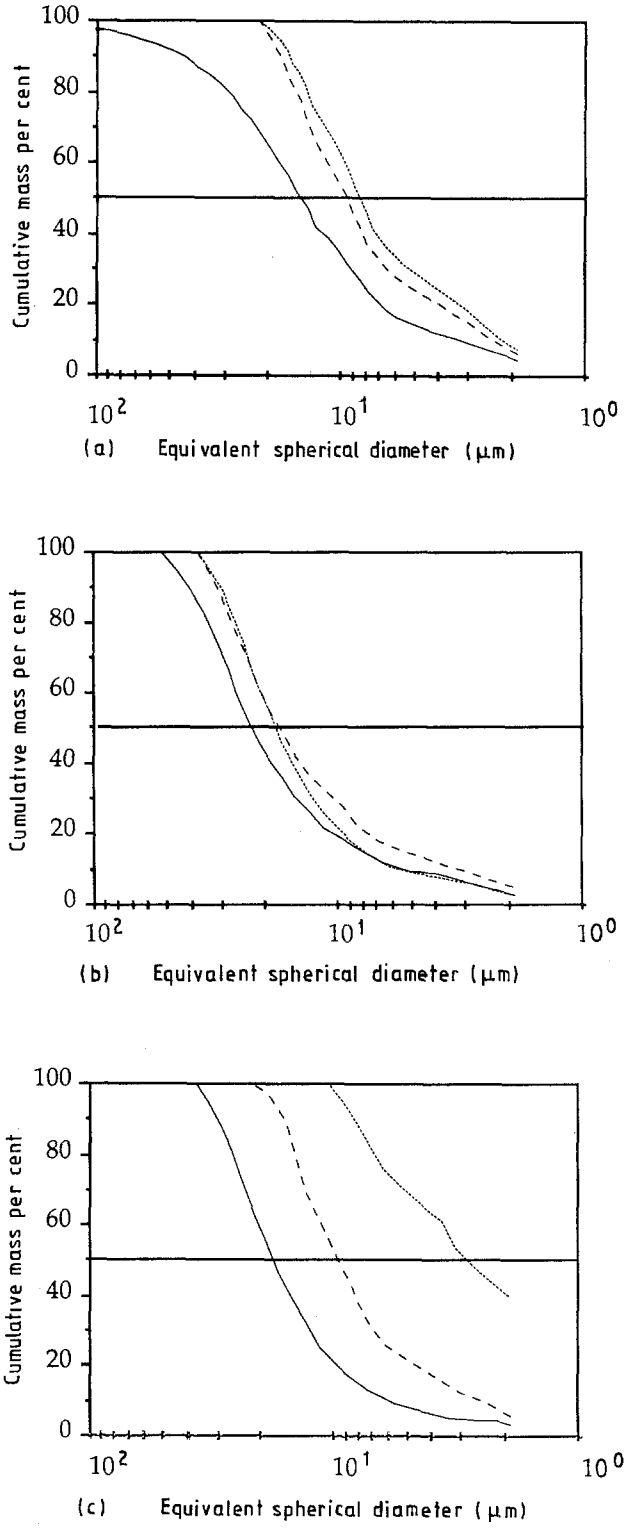

Figure 2 Agglomerate sizes of the different samples; cumulative frequency curves. (a) (——) 1, (---) 2, (– – –) 3; (b) (---) 4, (——) 5, (– – –) 6; (c) (——) 7, (---) 8, (– – –) 9.

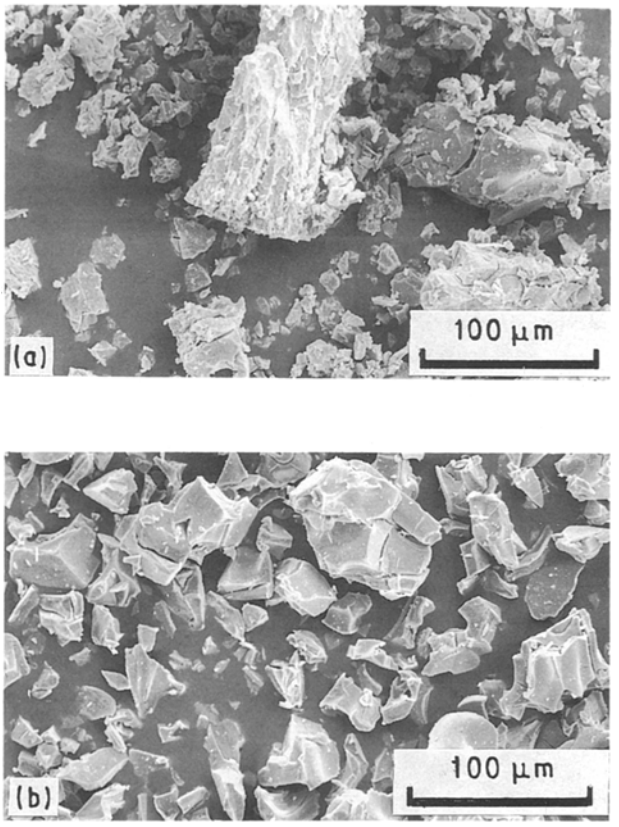

Figure 3 Electron micrographs of powders (a) 1 and (b) 4.

ceeding 2 μm. For Samples 4, 5 and 6, the distribution is slowly shifted towards large sizes, as the amount of yttrium oxide increases from 2.5 mol % to 3.5 mol %.

Samples 8 and 9 were intermediate between the two groups. They presented only one kind of pore corresponding, probably, to an interaggregates porosity as for Samples 4, 5 and 6, but their specific surface area was five-fold greater (1.1 $m^2\ g^{-1}$ for Sample 9) and their pore size very much smaller (0.75 μm for Sample 9).

3.3. Radiocrystallographical analysis

For Samples 4, 5, 6, 7, 8 and 9, the X-ray diffraction patterns indicate only tetragonal zirconia, whereas for Samples 1, 2 and 3, the peaks of monoclinic zirconia are also present. The ratio of monoclinic phase obtained by comparing the intensities of peaks (1 1 1) and (1 1 $\bar{1}$) for the monoclinic phase and (1 1 1) for the tetragonal one, according to Fillit *et al.*'s method [5], are given in Table III.

TABLE II Porosity characterization of Samples 4, 5, 6 and 7

Sample	Total porous volume ($mm^3\ g^{-1}$)	Specific surface area ($m^2\ g^{-1}$)	Pore size (μm)	Peak maximum (μm)
4	117	0.19	0.30–3.75	2.0
5	125	0.14	0.30–5.00	2.3
6	120	0.17	0.30–7.50	3.5
7	114	0.22	0.25–5.00	2.0

TABLE III X-ray analysis of zirconia samples

	Sample								
	1	2	3	4	5	6	7	8	9
Volumic fraction of monoclinic phase (%)	24	30	18	0	0	0	0	0	0

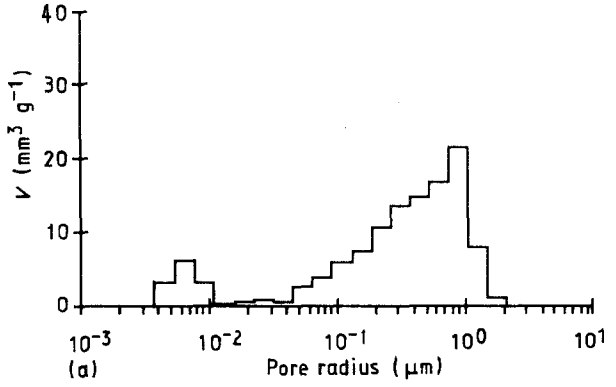

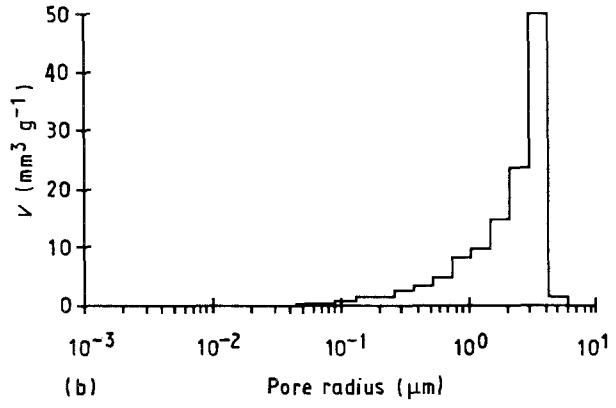

Figure 4 Pore-size distribution of Samples (a) 1 and (b) 6.

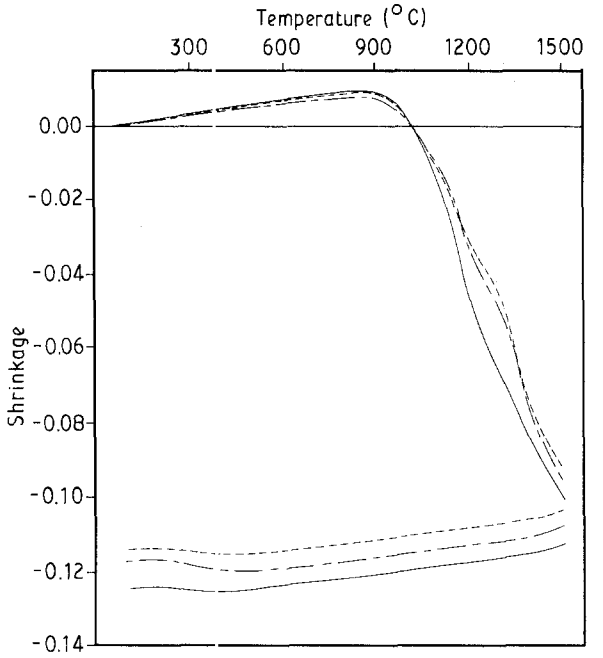

Figure 5 Dilatometric curves of Samples (– – –) 1, (— – —) 2 and (——) 3.

4. Dilatometric and thermogravimetric behaviour of the samples

4.1. Dilatometric behaviour

As for porosity measurements, the dilatometric behaviour of samples was investigated on pellets prepared by uniaxial pressing at 400 MPa. The curves were recorded under static air with a heating rate of 150 °C h^{-1}.

The powders of the first group exhibit two different types of behaviour.

(i) Curves recorded for Samples 1, 2 and 3 are identical (Fig. 5). A linear expansion is noticed up to 900 °C and then a progressive contraction (highest rates at 1160 and 1350 °C) which is incomplete at 1500 °C. The cooling curves show a destabilization phenomenon producing a volume increase due to the formation of monoclinic zirconia. The final linear shrinkages do not exceed 11.5%.

(ii) Curves recorded for Samples 4, 5 and 6 (Fig. 6) show a dedensification phenomenon, beginning at 1100 °C and occurring up to 1400 °C. Its intensity increases at the same time as the proportion of yttrium oxide increases. The destabilization phenomenon is no longer observed on the cooling curves. The final linear shrinkages fall to 7.5%.

The powder of the second group (Sample 7) is characterized by a dilatometric curve (Fig. 7) very similar to that of Sample 5, the final linear shrinkage being the same.

The dilatometric curves recorded for powders of the third group (Samples 8 and 9) exhibit neither destabilization, nor dedensification (Fig. 8). The densification arises more rapidly and the final linear shrinkage reaches a higher value for Sample 9 (14.5%) than for Sample 8 (10%).

Densities (green and sintered) are given in Table IV. Values obtained after sintering are always very far

from the theoretical one (6.1) even for Sample 9, still characterized by an important shrinkage.

Observation of the fracture of sintered pellets reveals, for all powders, essentially an intraaggregate sintering (Fig. 9). In Samples 4, 5, 6 and 7, the sizes of sintered aggregates, several tens of micrometres, are greater than in the other samples. Moreover, blisters and craters are formed at the surface of sintered aggregates.

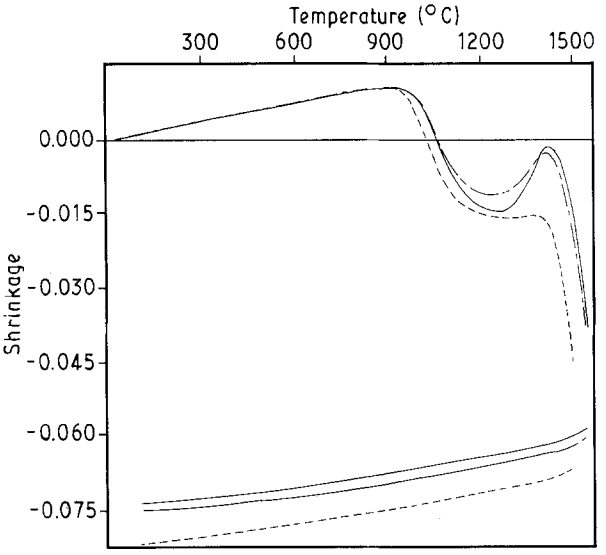

Figure 6 Dilatometric curves of Samples (– – –) 4, (— – —) 5, and (——) 6.

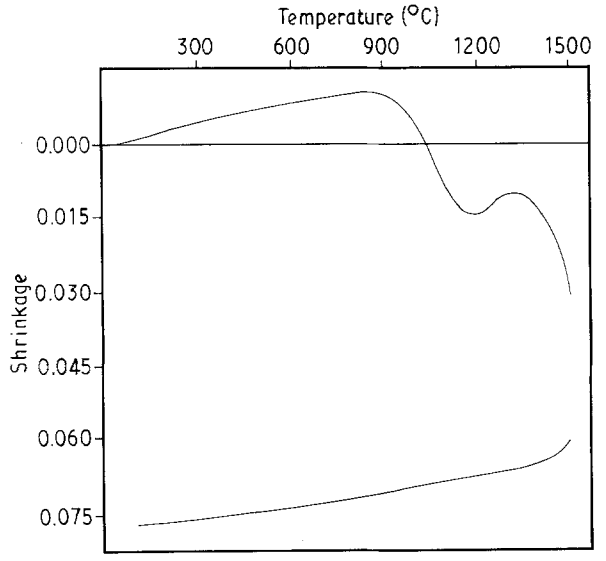

Figure 7 Dilatometric curve of Sample 7.

4.2. Powder thermogravimetric behaviour

The thermogravimetric curves of Samples 2, 3, 4, 6 and 8, recorded under the same conditions as the dilatometric curves (Fig. 10), reveal two successive weight losses. The first, under 300 °C, shows that small amounts of water are adsorbed on zirconia powders resulting from the pyrolysis of acetates at 950 °C. The second begins at 900 °C and is finished at 1500 °C for Samples 2, 3 and 8, whereas for Samples 4 and 6 it starts above 900 °C, being later as the yttrium oxide content increases, and is incomplete at 1600 °C. This second weight loss indicates that zirconia still contains removable species which lead to the formation of gaseous compounds.

5. Discussion

Among the nine powders, Samples 1, 2 and 3 present a

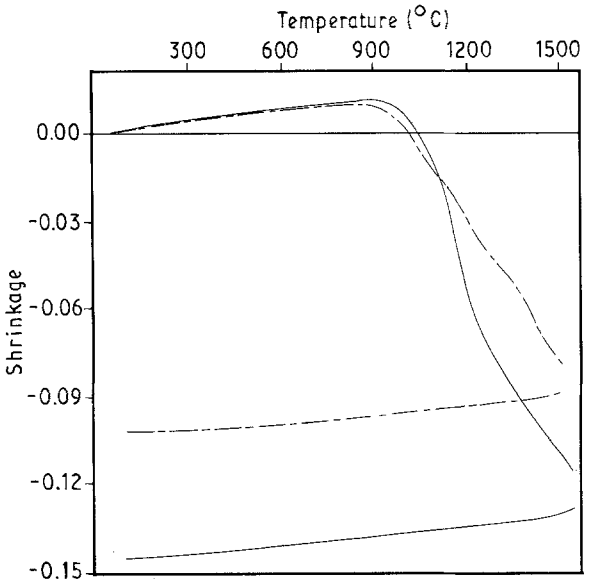

Figure 8 Dilatometric curve of Samples (— – —) 8 and (——) 9.

TABLE IV Dilatometric behaviour of zirconia samples

Sample	Green density	Sintering temperature (°C)	Sintered density	Shrinkage (%)	Expansion due to the phase change (%)
1	3.28	1500	4.49	11.5	0.5
2	3.2	1500	4.45	12	0.4
3	3.27	1500	4.7	12.5	0.6
4	3.33	1500	4.1	8.3	–
5	3.32	1550	3.97	7.5	–
6	3.38	1550	4	7.5	–
7	3.38	1500	4.09	7.8	–
8	3.43	1500	4.75	10	–
9	2.86	1500	4.58	14.6	–

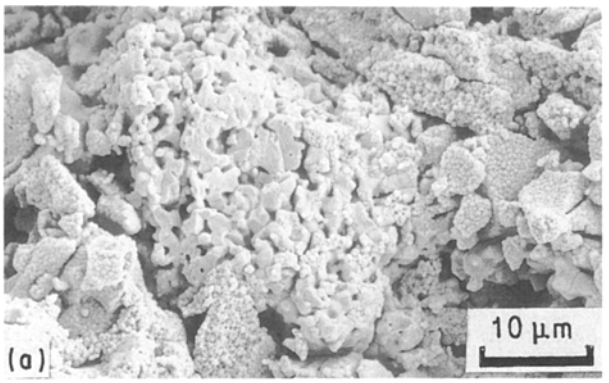

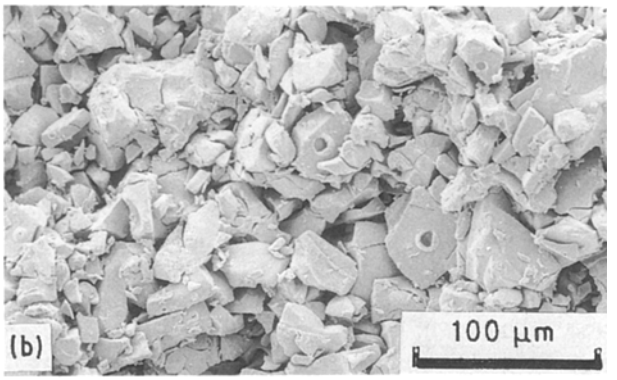

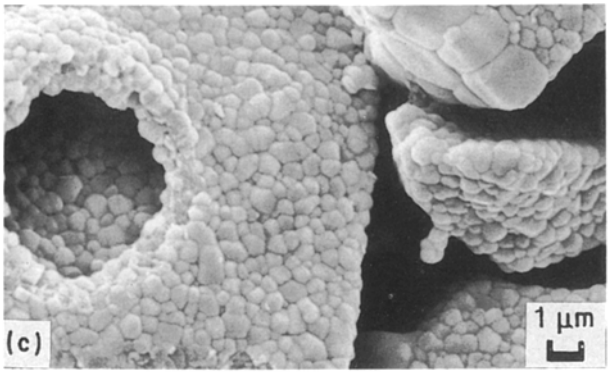

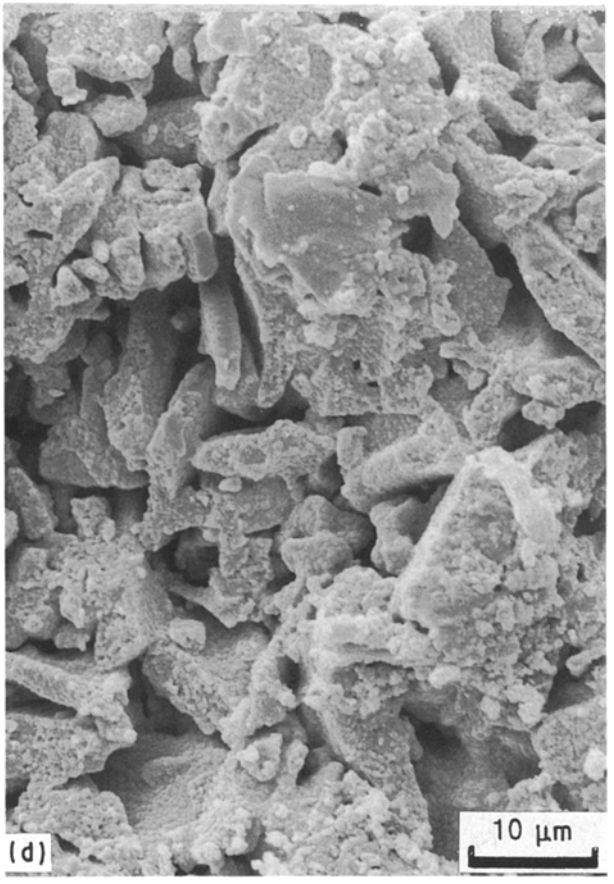

Figure 9 Scanning electron micrographs of a fracture of sintered Samples (a) 1, (b, c) 4 and (d) 9.

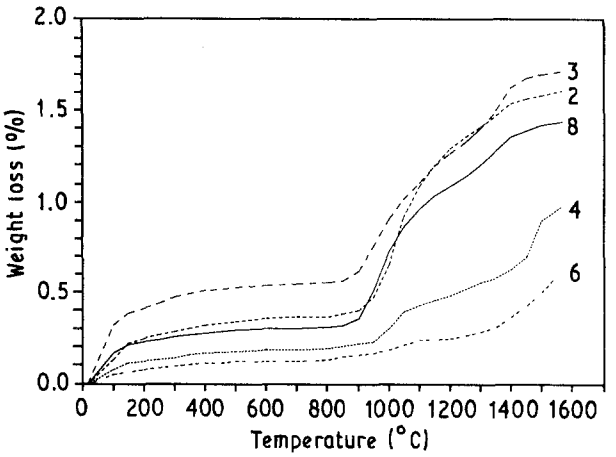

Figure 10 Thermogravimetric behaviour of Samples 2, 3, 4, 5, 6 and 8.

destabilization during cooling, Samples 4, 5, 6 and 7 a dedensification during heating and Samples 8 and 9 neither one nor the other phenomenon. It is noticeable that the dedensification occurs only for samples, which were pyrolysed in the muffle furnace with a non-linear heating rate (faster heating at low temperatures, slowing down when approaching 950 °C). Such a treatment leads to powders characterized, particularly for Samples 4, 5 and 6, by an interaggregate porosity with wide pores (2–3 µm). The porous volume is very badly distributed in the bulk of the aggregates, leading to specific surface areas lower than 0.2 $m^2 g^{-1}$ and to relatively high green densities. The aggregates seems to be more and more dense and large as the amount of yttrium oxide increases. The thermogravimetric behaviour shows that, for these samples the gaseous release shown by the second weight loss appears at higher temperatures than for the other powders. So, it is thought that, owing to the nature of the porosity, the gaseous compound formed locally during heating is trapped inside the sintered aggregates, inducing first an inflation of the sample explaining the dedensification on the dilatometric curves and the presence of blisters on fractures of sintered solids. When the pressure becomes high enough, the blisters burst producing craters, thus allowing gas release.

The pyrolysis of the other samples, performed with a 150 °C h^{-1} linear heating rate, gives powders characterized, especially for Samples 1, 2 and 3, by larger specific surface areas and bimodal pore distributions, including wide pores corresponding to the interaggregate porosity, and narrower pores due to an open intraaggregate porosity. This fine porosity, well dispersed in the bulk of the aggregates allows a regular

and earlier elimination of the gaseous compounds formed during sintering, avoiding a dedensification.

As for the destabilization, this is observed for Samples 1, 2 and 3 prepared in the same way as Samples 4, 5 and 6, by at first diluting the commercial starting concentrated zirconyl acetate solution in pure acetic acid, but differing only in the pyrolysis treatment. This no longer happens for Samples 8 and 9 synthesized by diluting zirconyl acetate in water and calcining the acetate powder with a 150 °C h^{-1} linear heating rate, as for Samples 1, 2 and 3. Thus the dilution in acetic acid is insufficient to explain by itself the destabilization, and the pyrolysis with a non-linear heating rate no more. Both factors must occur together. It is noticeable that the presence of monoclinic zirconia was indicated by X-ray diffraction only in these three samples. This could be explained by an inhomogeneous repartition of yttrium in the bulk of zirconia. The lower stabilization of powders could also result from crystallites exhibiting a size greater than a critical value, d_c, in the range 0.6–1.2 μm according to Leriche, *et al.* [6]. They are liable to induce the growth of large grains during sintering which might undergo the tetragonal to monoclinic transformation during cooling causing, in agreement with Smith and Baumard [7], an expansion.

6. Conclusion

Using the acetate route for yttrium-stabilized zirconia powder synthesis, it is necessary to carry out the pyrolysis with a sufficiently slow linear heating rate, especially at the beginning of the decomposition, in order to obtain a fine porosity allowing regular gaseous release and avoiding dedensification. Moreover, it seems preferable to dilute concentrated starting zirconyl acetate solution in water, especially because this procedure reduces the amount of ammonia solution necessary to raise the pH to 7. Under these conditions, a regular shrinkage is noticed during sintering but only poor density values are obtained owing to an absence of interaggregate sintering. Before considering powder milling, the present studies of the acetate production and principally the pyrolysis procedure, should be further developed with the purpose of decreasing the aggregation state of the powders.

7. References

1. A. SAMDI, T. GROLLIER BARON, B. DURAND and M. ROUBIN, *Ann. Chim. Sci. Mater.* **13** (1988) 171.
2. *Idem, ibid.* **13** (1988) 471.
3. *Idem, ibid.* **13** (1988) 517.
4. *Idem, ibid.* **13** (1988) 483.
5. R. FILLIT, P. HOMERIN, J. SCHAFFER, H. BRUYAS and F. THEVENOT, *J. Mater. Sci.* **22** (1987) 3566.
6. A. LERICHE, G. MOORTGAT, F. CAMBIER, P. HOMERIN, F. THEVENOT, G. GRANGE and G. FANTOZZI, in "Advances in Ceramics", Vol. 24 edited by S. Somiya, N. Yamamota and H. Yanagida, "Science and Technology of Zirconia III", (American Ceramic Society, 1988) p. 1033.
7. A. SMITH and J. F. BAUMARD, *Amer. Ceram. Soc. Bull.* **66** (1987) 1144.

Received 2 January
and accepted 29 October 1992